Bull. Mater. Sci., Vol. 34, No. 5, August 2011, pp. 1083–1087. © Indian Academy of Sciences.

Room-temperature ferromagnetic properties of Cu-doped ZnO rod arrays

C H XIA*, C G HU†, C H HU, Z PING and F WANG
Science College of Chongqing Jiaotong University, Chongqing 400074, People's Republic of China
†Department of Applied Physics, Chongqing University, Chongqing 400044, People's Republic of China

MS received 23 October 2010; revised 22 December 2010

Abstract. **We have investigated properties of the Cu-doped ZnO crystalline film synthesized by the hydrothermal method. X-ray diffraction and X-ray photoelectron spectroscopy results provide the evidence that Cu^{2+} is incorporated into the ZnO lattices. Photoluminescence spectrum of the rod arrays shows that the UV emission peak shifts a little to lower energy and its intensity decreased. There are another two emission peaks centred in blue and green regions because of the incorporation of Cu^{2+} ions. The rod arrays have exhibited room-temperature ferromagnetic behaviour with the remanence of $0{\cdot}926 \times 10^{-3}$ emu/cm^3. We suggest that the exchange interaction between local spin-polarized electrons (such as the electrons of Cu^{2+} ions) and conductive electrons is the cause of room-temperature ferromagnetism.**

Keywords. **Cu-doped ZnO; hydrothermal method; optical property; magnetic property.**

1. Introduction

Diluted magnetic semiconductors (DMSs) (Furdyna and Kossut 1988) are currently receiving intense theoretical and experimental attention because of the central role they may play in the emerging field of spin electronics (spintronics). DMSs are semiconducting alloys whose lattice is made up in part of substitutional magnetic atoms in which new functions can be added by transforming and controlling the types of spin states. These DMSs are potential candidates for technological applications in optoelectronics, magnetoelectronics, and microwave devices (Kin *et al* 2004; Bouloudenine *et al* 2005). Recently, theoretical investigations have suggested that wide bandgap semiconductors are the most promising candidates for achieving high Curie temperatures (Dietl *et al* 2000), which have been supported by *ab initio* calculations based on the local density. Among them, TM-doped ZnO compound semiconductors have been extensively studied, where TM is 3*d* transition metal such as Fe, Co, Ni, Mn etc. The presence of TM ions in these materials leads to an exchange interaction between itinerant *sp*-band electrons or holes and the *d*-electron spins localized at the magnetic ions, resulting in versatile magnetic-field-induced functionalities. Thereafter, remarkable progress has been made on realization of transition metal-doped ZnO (ZnO : TM) such as ZnO : Mn (Sharma *et al* 2003), ZnO : Co (Ueda *et al* 2001), ZnO : Fe (Han *et al* 2002) with T_c at or above room temperature (*RT*). However, from the experimental point of view, there are still questions about whether ferromagnetic ordering arises from the magnetic ions actually substituting in the lattice or from the secondary phases or metal precipitates. These questions motivated some researchers to investigate Cu-doped ZnO system (Hou *et al* 2007a, b), as Cu is a potential magnetic ion with a total spin of 1/2 by Hund's rule. The Cu-related secondary phases are antiferromagnetic which may make the interpretation of ferromagnetism in ZnO : Cu easier (Wei *et al* 2005). In this paper, we have synthesized Cu-doped ZnO rod arrays on Zn foils using a facile hydrothermal method. The as-synthesized samples were characterized by X-ray diffraction (XRD) and scanning electron microscopy (SEM). The constituents and the valence states of the Cu-doped ZnO were investigated by X-ray photoelectron spectroscopy. Photoluminescence spectra were used to analyse the existence of defects and impurities of the arrays after being doped with Cu. The magnetic properties of the Cu-doped ZnO rod arrays have been investigated at room temperature and cause of the magnetic properties has been discussed in detail. The results may provide some useful data for the theorists in DMS research.

2. Experimental

2.1 *Material preparation*

The ZnO cone arrays were synthesized through the hydrothermal method. Typically, a piece of high purity zinc foil and 1 mmol NaCl were put in a 25 mL autoclave vessel with 20 mL deionized water. Then, the vessel was put into a furnace preheated to 180°C. After reacting for 24 h,

*Author for correspondence (xxhkaixin@163.com)

the vessel was taken out and allowed to cool down to room temperature. The ZnO cone arrays growing on the surface of zinc foil was obtained after washing with deionized water. The Cu-doped ZnO rod arrays were obtained by retreatment of the as-prepared ZnO cone arrays with 1·0 mmol $CuCl_2$ in an autoclave vessel with 20 mL deionized water at 180°C for 24 h.

2.2 *Characterization*

XRD, EDS and XPS were used to investigate the crystalline phase and chemical composition of Cu-doped ZnO. SEM was used to characterize morphology and size of the synthesized samples. The PL spectra were measured at room temperature using SPEX Flurolog-2 spectrofluorometer.

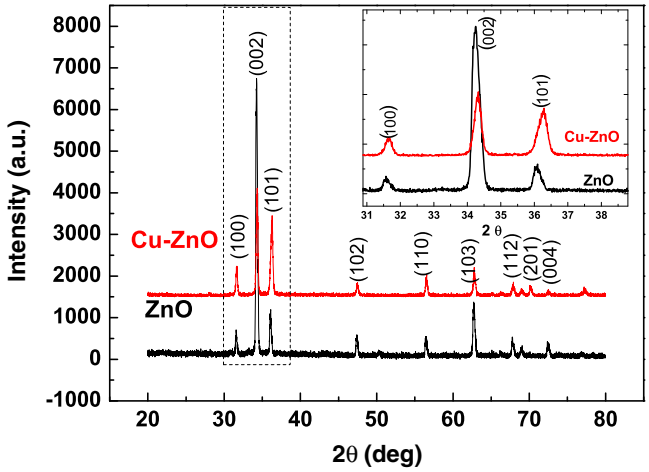

Figure 1. XRD patterns of undoped ZnO and Cu-doped ZnO sample (inset is enlarged part of rectangle region in figure 1).

2.3 *Magnetic measurement*

Magnetic measurements were carried out using ADE magnetics Model Ev 11 Vibrating Sample Magnetometer. The magnetic hysteresis loop was observed in the range of $-10{,}000$ Oe $< H <$ 10,000 Oe at a temperature of 293 K.

3. Results and discussion

3.1 *XRD analysis*

XRD patterns of undoped ZnO and Cu-doped ZnO are shown in figure 1. All the peaks of undoped ZnO are assigned by using the JCPDS file (No. 89-0511), a pure hexagonal phase with lattice constant $a = 0{\cdot}3249$ nm and $c = 0{\cdot}5205$ nm. Comparing the peaks of pure ZnO with that of Cu-doped ZnO, we found that all peaks belonged to the hexagonal lattice of ZnO with no indication of secondary phase such as Cu_5Zn_8 or CuZn, indicating that Cu ions might have entered into the ZnO lattices. However, we observed a slight shift of diffraction peaks to larger angle from the inset. This result indicates decreased lattice parameters because the ionic radius of Cu^{2+} (72 pm) is slightly larger than that of Zn^{2+} (60 pm) (Samanta *et al* 2007).

3.2 *Microstructure*

Figure 2 shows SEM images of the undoped ZnO (a) and Cu-doped ZnO (b). From figure 2a, we find that the morphology of pure ZnO looks like cone arrays. The cone arrays change into rod arrays with spire ends after being doped with Cu. Figure 3 is the EDS of the undoped ZnO (a) and the Cu-doped ZnO (b). The EDS shows the existence of Cu ions in the Cu-doped ZnO.

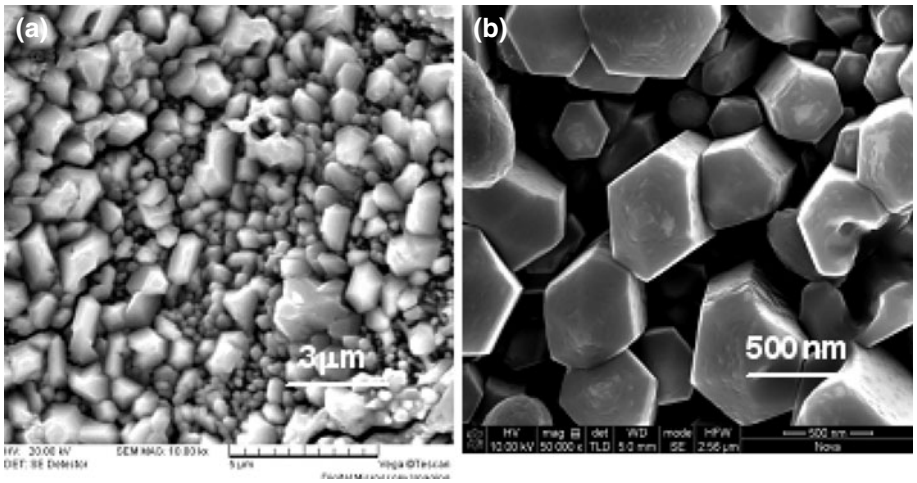

Figure 2. (**a**) SEM images of undoped ZnO cone arrays and (**b**) Cu-doped ZnO rod arrays.

3.3 *X-ray photoelectron spectra (XPS)*

The constituents and valence states at the surface were investigated by XPS. All binding energies have been corrected for the charging effect with reference to the C 1*s* line at 284·6 eV. The survey spectrum of the sample (figure 4a) showed peaks corresponding to Zn, Cu, O, and C, ruling out incorporation of any additional impurities during sample preparation. Figure 4b shows the Zn 2*p* core level peaks in the XPS spectrum, and it clearly proves that the zinc exists as the Zn^{2+} oxidation state in the film (Hlaing *et al* 2009). Figure 4c shows the high resolution spectra of the Cu 2*p* peaks. The typical

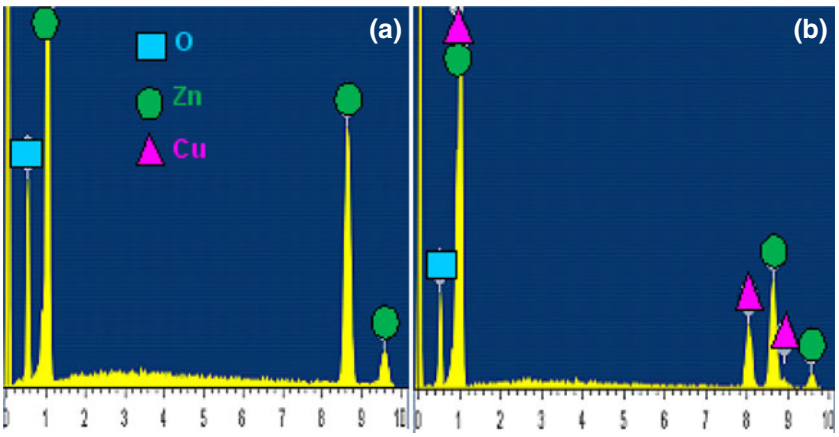

Figure 3. (**a**) EDS of undoped ZnO and (**b**) Cu-doped ZnO sample.

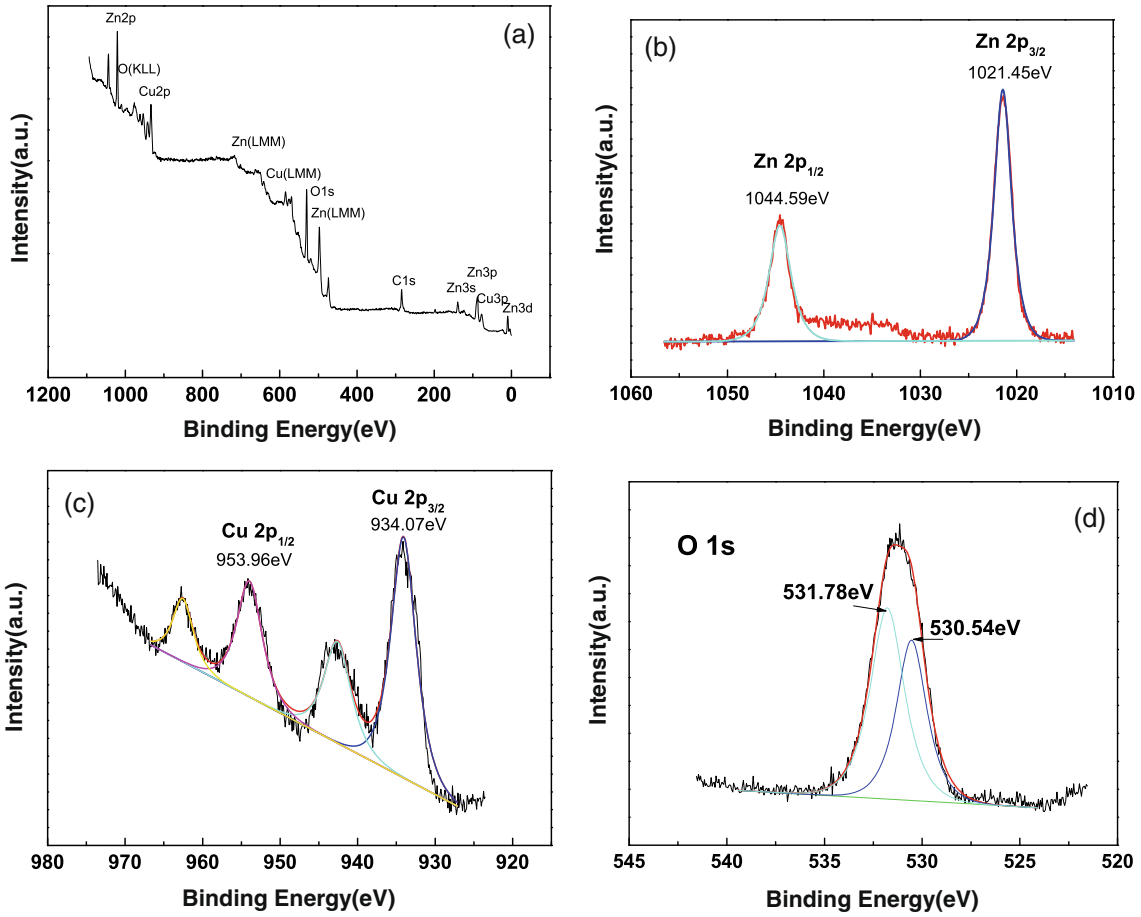

Figure 4. XPS integral spectra (**a**), Zn2*p* (**b**), Cu2*p* (**c**) and O1*s* (**d**) core-level XPS spectrum for Cu-doped ZnO sample.

fingerprint with four peaks appeared in the Cu 2p spectrum. The presence of two additional satellite bands in the 941–946 and 961–965 eV regions depends on removal of the degeneration that occurs when the copper electronic configuration is unsaturated d^9 (Cu^{2+}), thus allowing p–d hybridization (Meda *et al* 2002). On the contrary, when copper reaches the electronic configuration d^{10} (Cu^{+}), the satellite bands disappear and only two peaks are visible in the copper spectrum as reported by Chakraborti *et al* (2007). It is confirmed that Cu ions were in a divalent state in the sample. The typical O 1s peak in figure 4d can be consistently fitted by two nearly Gaussian curves centred at 530·54 and 531·78 eV. The peak centred at 530·54 eV (the lower binding energy) in the O 1s spectrum is attributed to O^{2-} ions on wurtzite structure of hexagonal ZnO (Chen *et al* 2000). And the peak centred at 531·78 eV (the higher binding energy) is associated with O^{2-} ions in the oxygen deficient regions within the matrix of ZnO (Fan and Goodenough 1977). This phenomenon indicates that there are some oxygen vacancies in this sample.

3.4 *Optical analysis*

In order to further determine the cause of ferromagnetism, we measured the PL spectrum of the Cu-doped ZnO samples. The room temperature PL spectra on both the Cu-doped and undoped ZnO samples are shown in figure 5. The differences in the PL spectra are observed between them. Only a UV emission peak can be observed without any significant emission in visible region on the pure ZnO cone arrays, though the green emission is often observed in many reports (Vanheusden *et al* 1996, 1998; Kong *et al* 2001; Yang *et al* 2008). The UV emission is attributed to the near-band-edge emission from the recombination of free excitons through an exciton–exciton collision process (Richardson and Milligan 1956; Schwartz *et al* 2004). After Cu ion incorporation, the UV emission peak shifts a little to lower energy with decreased intensity. Besides, we can see there are two emission peaks centred at about 469 nm (2·64 eV) and 535 nm (2·32 eV), respectively. The blue emission might come from the intrinsic defects or / and Cu impurity. Zn interstitial (Zn_i) and oxygen vacancy (V_O) are main donor defects while Zn vacancy (V_{Zn}) and oxygen interstitial (O_i) are main acceptor defects in intrinsic ZnO (Peng *et al* 2008). Cu behaves as an acceptor level with a deep energy of ∼0·17 eV below the conduction band (Pearton *et al* 2005). Sun (2000) calculated energy levels of the intrinsic defects in ZnO films. The energy interval from the level of interstitial Zn (Zn_i) to zinc vacancy (V_{Zn}) is 2·62 eV (473 nm). According to his calculations, we think that the blue emission centred at 469 nm corresponds to the electron transition from the level of interstitial Zn (Zn_i) to the zinc vacancy (V_{Zn}), as some of Cu ions partially substitute the Zn ions in ZnO crystal lattice, and meanwhile, the Zn ions released from the lattice must have entered into the interval of the lattice to form the interstitial zinc (Zn_i) defects. The oxygen vacancies in ZnO lattices lead to the green emission (Zhang *et al* 2001) centred at 535 nm.

3.5 *Magnetic properties*

Figure 6 shows the magnetic hysteresis ($M-H$) curves measured from −10,000 to 10,000 Oe at 293 K for the pure ZnO and Cu-doped ZnO samples. Obviously, the pure ZnO shows paramagnetism at room temperature. The ferromagnetic hysteresis loops are clearly observed from the $M-H$ curves for the Cu-doped ZnO samples. The remanence (M_r) is $0{\cdot}926 \times 10^{-3}$ emu/cm^3, and the coercive field (H_c) is 23 Oe for the sample. The Cu-related secondary phases are antiferromagnetic, so we think the ferromagnetism is intrinsic. According to the Ruderman–Kittel–Kasuya–Yosida (RKKY) theory (Ruderman and Kittel 1954; Yosida 1957), the

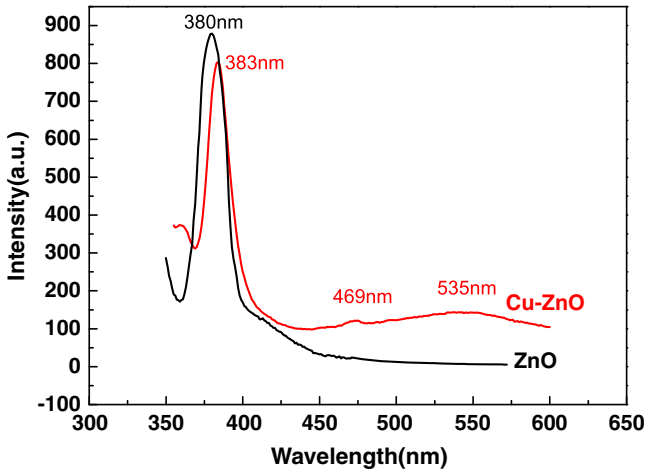

Figure 5. Room temperature photoluminescence spectra of pure ZnO and Cu-doped ZnO samples.

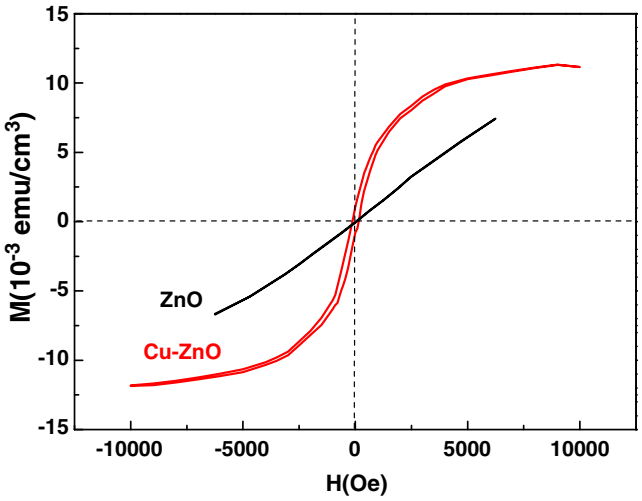

Figure 6. Hysteresis loop of pure ZnO and Cu-doped ZnO samples at a temperature of 293 K.

exchange interaction between local spin-polarized electrons (such as the electrons of Cu^{2+} ions) and conductive electrons is the main cause that leads to the ferromagnetism. This interaction brings about the spin polarization of conductive electrons. Subsequently, the spin-polarized conductive electrons have an exchange interaction with local spin-polarized electrons of Cu^{2+} ions. Thus, after the long-range exchange interaction, almost all Cu^{2+} ions exhibit the same spin direction. The conductive electrons are regarded as a media to contact all Cu^{2+} ions.

4. Conclusions

Cu-doped ZnO rod arrays can be obtained through the hydrothermal method. Cu ions are incorporated into the ZnO lattices as Cu^{2+} ions. Two additional emission peaks centred at about 469 nm and 535 nm were observed in PL spectra. The rod arrays exhibit room-temperature ferromagnetic behaviour with a remanence of $0{\cdot}926 \times 10^{-3}$ emu/cm^3. We think the ferromagnetism is intrinsic, as the Cu-related secondary phases are antiferromagnetic. The ferromagnetism at room temperature is a result of the exchange interaction between local spin-polarized electrons (such as the electrons of Cu^{2+} ions) and conductive electrons according to the Ruderman–Kittel–Kasuya–Yosida theory.

Acknowledgements

This work was supported by the NSFC (60976055), Postgraduates' Innovative Training Project (S-09109) of the 3rd-211 Project, and the large-scale equipment sharing fund of Chongqing University.

References

Bouloudenine M, Viart N, Colis S, Kortus J and Sinia A 2005 *Appl. Phys. Lett.* **87** 052501

Chakraborti D, Trichy G R, Prater J T and Narayan J 2007 *J. Phys. D: Appl. Phys.* **40** 7606

Chen M, Wang X, Yu Y H, Pei Z L, Bai X D, Sun C, Huang R F and Wen L S 2000 *Appl. Surf. Sci.* **158** 134

Dietl T, Ohno H, Matsukura F, Cibert J and Ferrand D 2000 *Science* **287** 1019

Fan J C C and Goodenough J B 1977 *J. Appl. Phys.* **48** 3524

Furdyna J K and Kossut J (eds) 1988 *Semiconductors semimetals* (New York: Academic)

Han S J, Song J W, Yang C H, Park S H, Park J H, Jeong Y H and Rhie K W 2002 *Appl. Phys. Lett.* **81** 4212

Hlaing Oo W M, Saraf L V, Engelhard M H, Shutthanandan V, Bergman L, Huso J and McCluskey M D 2009 *J. Appl. Phys.* **105** 013715

Hou D L, Ye X J, Zhao X Y, Meng H J, Zhou H J, Li X L and Zhen C M 2007a *J. Appl. Phys.* **102** 033905

Hou D L, Ye X J, Meng H J, Zhou H J, Li X L, Zhen C M and Tang G D 2007b *Appl. Phys. Lett.* **90** 142502

Kin Y M, Yoon M, Park I W and Lyou J H 2004 *Solid State Commun.* **129** 175

Kong Y C, Yu D P, Zhang B, Fang W and Feng S Q 2001 *Appl. Phys. Lett.* **78** 407

Meda L, Ranghion G, Moretti G and Cerofolini G F 2002 *Surf. Interface Anal.* **33** 516

Pearton S J, Norton D P and Ip K 2005 *Prog. Mater. Sci.* **50** 293

Peng X P, Xu J Z, Zang H, Wang B Y and Wang Z G 2008 *J. Lumin.* **128** 297

Richardson J T and Milligan W O 1956 *Phys. Rev.* **102** 1289

Ruderman M A and Kittel C 1954 *Phys. Rev.* **96** 99

Samanta K, Dussan S and Katiyar R S 2007 *Appl. Phys. Lett.* **90** 261903

Schwartz D A, Kittilatved K R and Gamelin D R 2004 *Appl. Phys. Lett.* **85** 1395

Sharma P, Gupta A, Rao K V, Owens F J, Sharma R, Ahuja R, Osorio Guillen J M, Johansson B and Gehring G A 2003 *Nat. Mater.* **2** 673

Sun Y M 2000 *Study on the Synthesis and Physical Properties of ZnO-based Diluted Magnetic Semiconductors*, Ph.D. thesis, University of Science and Technology of China, China

Ueda K, Tabata H and Kawai T 2001 *Appl. Phys. Lett.* **79** 988

Vanheusden K, Warren W L, Seager C H, Tallant D R, Voigt J A and Gnade B E 1996 *J. Appl. Phys.* **79** 7983

Vanheusden K, Seager C H, Warren W L, Tallant D R and Voigt J A 1998 *Appl. Phys. Lett.* **68** 403

Wei M, Braddon N, Zhi D, Midgley P A, Chen S K, Blamire M G and MacManus-Driscill G L 2005 *Appl. Phys. Lett.* **86** 72514

Yang J H *et al* 2008 *J. Alloys Compd* **450** 508

Yosida K 1957 *Phys. Rev.* **106** 893

Zhang S B, Wei S H and Zunger A 2001 *Phys. Rev.* **B63** 075205